ISSN : 0974 - 7451 Volume 9 Issue 8

Environmental Science

An Indian Journal

Current Research Paper

ESAIJ, 9(8), 2014 [285-293]

Enhanced photovoltaic cell incorporating a dye-sensitized ZnS/ ZnO composite thin films

P.N.Prashanth Kumar[1], H.S.Bhojya Naik[1]*, H.R.Ravi[2], R.viswanath[1], H.R.Sreepad[3]

[1]Department of Industrial Chemistry, Kuvempu University, Shankaraghatta-577 451, (INDIA)

[2]Research Centre, PG Department of Physics, BETAHE, Bharthinagar, Mandya, (INDIA)

[3]Research Centre, PG Department of Physics, GFG College, Mandya, (INDIA)

E-mail : hsb_naik@rediffmail.com

ABSTRACT

The present paper reports that preparation of entacopone intermediate molecule (catacol sensitizer) and characterized by Mass spectra, IR spectra and melting point which exactly matches with the reported molecule. For improving the photovoltaic cell the ZnS was thermally evaporated onto conducting fiuorine-doped tin oxide glass; then a particulate ZnO layer was pasted and sintered to form a ZnS/ZnO composite layer. A visible light source was utilized to excite the Catacol sensitizer, which was adsorbed onto the surface of the ZnO and composite films. The ZnS layer is believed to provide an alternative pathway for electrons to move across ZnO barriers. This alternative pathway with the composite layer structure provides higher power efficiency than does a single layer of ZnO films.

KEYWORDS

Catacol sensitizer;
ZnO substrate;
ZnS/ZnO substrate;
Photovoltaic application.

INTRODUCTION

The design of molecular chromophores is critically important for the development of dye sensitized solar cells (DSSCs)[1,2] for photoelectricity and photocatalysis[3-6]. Since their breakthrough in 1991 as reported by Gratzel et.al, Ru-dye sensitized titanium dioxide (TiO_2) offers a respectably high power efficiency of around 10%[1], which raised the hope of fabricating a stable, highly efficient and electrochemical photovoltaic cell. Other metal oxides such as SnO_2, CdO, Nb_2O_5, Fe_2O_3, ZnO, and MgO have also been tested. Among them, ZnO has drawn much attention owing to its equal energy band level (3.0–3.2 eV) compared to that of TiO_2 and also in contrast to the above metal oxides[7]. Hagfeldt et al.[8] reported a promising efficiency of 5% using ZnO nanoparticles, which exhibited the feasibility of being an alternative option for TiO_2. On the other hand, other semiconductors showing lower efficiency than TiO_2 have exhibited comparable values when used as composite films, such as SnO_2/MgO[9], CdS/MgO[5], ZnO/SnO_2[10], and (Cd, Zn)S/(Cd, Zn)O[11]. In addition, due to the intrinsic instability in acid ambient, the ZnO nanoparticles were vulnerable to the ruthenium based dyes. Moreover, the dyes containing complexing agents can also detach the Zn^{2+} from the host lattice to generate Zn^{2+}-dye agglomerations at the interface, resulting in low injection efficiency and high recombination rate[12–

14]. The modification of another protecting layer (like SiO_2, Al_2O_3, TiO_2 and ZnS) could indeed enhance the stability of ZnO surface and suppress the recombination[15–19]. However, it would inevitably bring forth injection problem and extra fabrication cost[20]. Therefore, there are still many challenges to promote the PCE of ZnO based DSSCs.

One of our idea is to reduce the recombination rate is to create core shell heterostructures. The energy barrier formed between the core and shell materials can hinder the recombination process[15]. The oscillator strength for such a transition would be small for two semi bulk slabs, but in nanometer-scaled structures, the spatial proximity of the band-edge wave functions to interface would lead to an increase in the oscillator strength. Thus, it is critically important to know how the energy band gap can be in these structures and how large the absorption can be obtained these composite films. In this way we were encouraged by the variety of efficient experimental methods for the partial conversion of ZnO nanofilms into ZnO/ZnS nano composite films[21-27]. The optical properties of the ZnS layer show remarkable infiuence on the final performance of the DSSCs, which indicates that the conversion efficiency can be further improved by careful design of the photoanode materials i.e. the conversion efficiency of ZnO-based DSSCs is the recombination of the electrons injected into the ZnO with either the dye or the redox electrolyte, thereby reducing the cell efficiency[28]. Thus, a ZnS/ZnO composite thin film was fabricated in order to improve the performance of a cell based on the weakly dye-adsorbing ZnS. To fabricate ZnS thin films many methods have been used such as screen printing and sintering[29], electrochemical deposition[30,31], chemical bath deposition[32], thermal evaporation[33], MOCVD[34] and sputtering. In this work we have demonstrated thermal evaporation processes were used to deposit the ZnS on ITO films.

The other objective of this work is to improve light absorption efficiency of dye-sensitized solar cells. Especially increased interest in organic dye sensitizers that have resulted in intensive study of their function in DSSCs. Conjugated organic dyes offer several advantages over metal containing dyes as photosensitizer, such as (1) potential for low cost production (no precious metals needed), (2) large absorption coefficient in the visible spectral region due to strong π to π* transitions and molecular design may be used to search for better absorption efficiencies and redox potentials. Efficiency of DSSCs using organic sensitizers are still clearly below when comparied to that of using ruthenium sensitizers, which have shown record conversion efficiency of 11%. The major drawback of organic photosensitizers is, their relatively low spectral bandwidth in the visible or near-infrared regions, as well as their relatively low resistance toward photodegradation. In the past years, organic dyes have got particular attention and have been tested as photosensitizers, such as eosin Y[35], ribofiavin[36], cyanine[37], cresyl violet[38], merocyanine[39]. coumarin[40] and xanthenes[41]. The chosen dyes possessing carboxylate or hydroxyl functional groups that enable the direct interaction with the surface of TiO_2 particles, thereby providing a path for electron transfer from the excited dye adsorbate to the semiconductor[40].

In the present work, we have select the novel molecule to adopt solar cell i.e. catacol sensitizer which is the intermediate compound of entacopone molecule (used for Parkinson disease). It is a new strategic molecular designs of organic dye in terms of engineering which is interface between the organic dye and the ZnO or ZnO/ZnS surface that required to improve the photovoltaic performance of organic DSSCs. The cell was fabricated with ZnS film by vapor deposition technique after introducing the ZnO onto the ZnS films by doctor blade technique to overcome the recombination rate.

EXPERIMENTAL SECTION

Materials and methods

$Zn(NO_3)_2.6H_2O$, PEG-2000 surfactant, 3,4-dihydroxy-5-nitrobenzaldehyde,2-cyanoacetic acid, piperidine, ZnS pellets, these organic and inorganic reagents were purchased from Himedia chemical laboratory of analytical grade, and needed no further purification. The counter platinum electrode was coated on ITO glass sheet by vacuum coating technique.

Spectral measurements

Mass spectra were recorded on LCMS-2010A SHIMADZU, UV-Visible spectrophotometer (UV-1650 PL Shimadzu, model) used to measure the optical properties IR spectra (nominal 4-cm^{-1} resolution) were measured using a Digilab FTS-40 spectrometer in which the dye powders were held in KBr pellets in the case of Entacopone intermediate (E_1) sensitizer ligand. The chemisorbed sensitizer on ZnO films were measured using an attenuated total reflectance (ATR) spectroscopy.

Synthesis of (2E)-2-Cyano-3-(3,4-dihydroxy-5-nirtrophenyl)prop-2-enoic acid [E_1]

A round bottom flask containing 3,4-dihydroxy-5-nitrobenzaldehyde (1 g, 5.4 mmol), 2-cyanoacetic acid (0.69 g, 8.2 mmol), piperidine (0.86 g, 1.0 mmol), acetic acid (0.42 g, 7 mmol), and ethanol (10 ml) were heated to reflux for 4 h. The reaction mixture was concentrated under reduced pressure and then diluted with ethyl acetate (10 ml) and water (10 ml). The resulting solution was basified with 10 % w/v aqueous sodium hydroxide solution (2 ml). The aqueous layer was separated and acidified with concentrated HCl (2 ml). The obtained precipitate was stirred for 1h at 5°C, filtered, and dried to the product (2E)-2-cyano-3-(3,4-dihydroxy-5-nirtrophenyl)prop-2-enoic acid with an yield of 0.8 g, 58 % and M.p. was observed as 124–126° C[42].

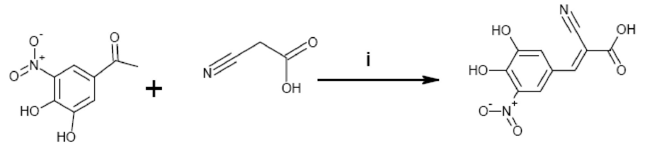

i) piperidine, CH_3COOH , ethanol ,80^{0}C

Scheme 1

Preparation of ZnS films

ZnS nanoparticles were heated at 3x10^{-5} Torr and condensed from the vapor phase onto the ITO glass substrate. The film thickness was maintained at around 50 nm which were deposited by thermal evaporation technique by Molybdenum (MO) boat. The glass substrates were cleaned by ethanol before deposition. The substrates were placed in a sample holder and kept at a distance of 18 cm from the vaporation source. The substrate holder was connected to an electric motor to rotate the substrate during the deposition to achieve uniform film. for vaporation the electric current was maintained at 150 Å. The nominal film thickness was controlled by an optical thickness monitor.

Preparation of ZnO and ZnO/ZnS films

The ZnO coating was obtained by pasting ZnO nanoparticles suspended in a propylene carbonate (PC) solution with a trace amount of surfactant (Triton X-100, Sigma) and sintering them at 450°C for 30min to remove the organic impurities between ZnO nanoparticles.In the following discussion, a simplified symbol is used to identify each sample. A slash "/" denotes the interface of each layer, and the dye is usually denoted by the layer next to ZnO. The thermally evaporated ZnS is simply denoted as "ZnS." A pure ZnO layer was obtained by pasting and sintering ZnO particles which is denoted as "ZnO". The composite film prepared in this study was obtained layer by layer, which differs from those of mixed layers as reported in the literature[7]. The purpose of the layered structure was to increase the adsorptive surface area offered by the ZnO. A ZnO seed layer was deposited onto ZnS coated fluorine-doped tin oxide (ITO) glass substrate using doctor blade technique. Then the synthesizing Catacol sensitizer was chemisorbed onto ZnO nanocrystalline or ZnO/ZnS nanocrystalline films by immersing this films into a E_1 ligand containing ethanol solution.

RESULT AND DISCUSSION

Mass spectra of (2E)-2-Cyano-3-(3,4-dihydroxy-5-nirtrophenyl)prop-2-enoic acid

The as synthesized high yield of (2E)-2-Cyano-3-(3,4-dihydroxy-5-nirtrophenyl)prop-2-enoic acid, its mass spectra m/z values of 249 (M-H) which exactly matches with the reported literature G. Srikanth. et.al[42].

XRD studies

The structural properties have been studies by X-ray diffraction technique using CuKα radiation source (λ=1.54056Å).The X-ray diffraction pattern shows that the composite film deposited onto ITO substrate as shown in Figure 2. The maximum peak were observed and matched with the JCPDS data. The structural parameters were calculated from the XRD pattern in which the film nature is wurtzite and hexagonal structure whose grain size were determined by using Debye-Scherer's formula is $D = 0.9\lambda/\beta \cos\theta$, Where D is the grain size, β is the FWHM of the diffraction peak, θ is the Bragg

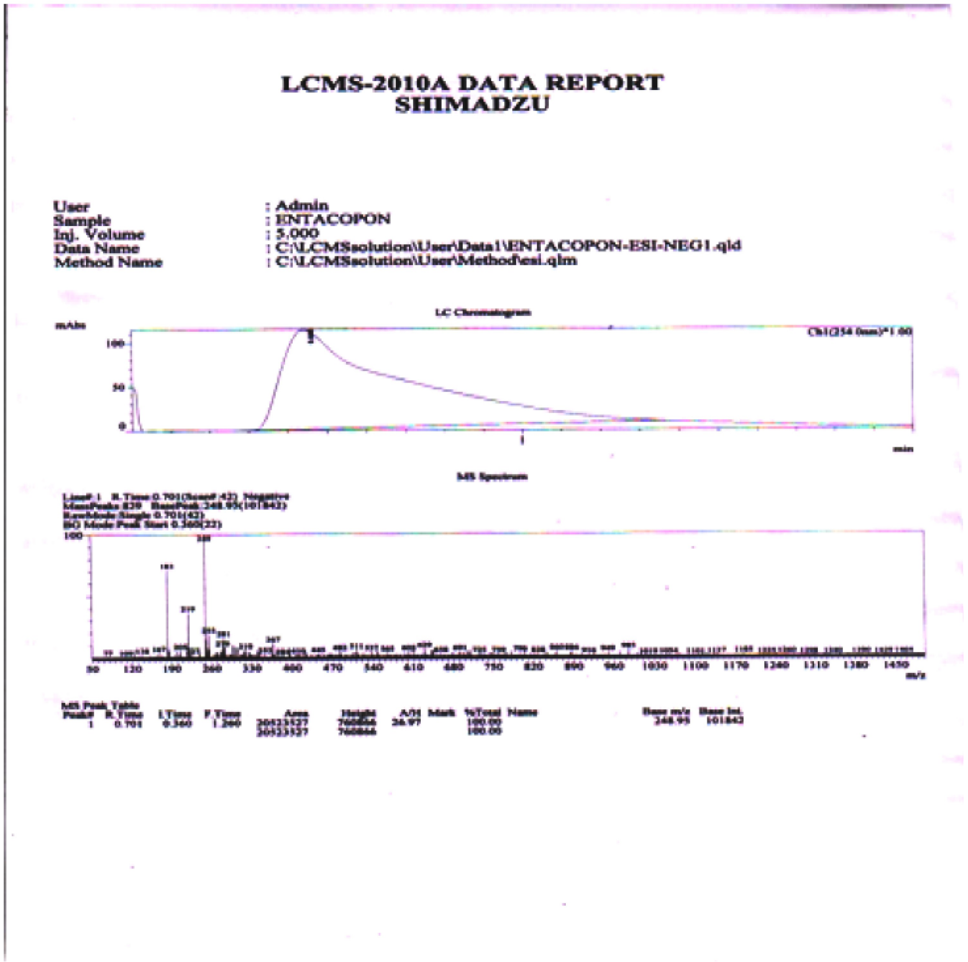

LCMS-2010A DATA REPORT
SHIMADZU

User : Admin
Sample : ENTACOPON
Inj. Volume : 5.000
Data Name : C:\LCMSsolution\User\Data1\ENTACOPON-ESI-NEG1.qld
Method Name : C:\LCMSsolution\User\Method\esi.qlm

Line#:1 R.Time:0.701(Scan#:42) Negative
MassPeaks:839 BasePeak:248.95(101842)
RawMode:Single 0.701(42)
BG Mode:Peak Start 0.360(22)

MS Peak Table

Peak#	R.Time	I.Time	F.Time	Area	Height	A/H	Mark	%Total	Name	Base m/z	Base Int.
1	0.701	0.360	1.260	20523527	760846	26.97		100.00		248.95	101842
				20523527	760846			100.00			

Figure 1 : Mass spectra of (2E)-2-Cyano-3-(3,4-dihydroxy-5-nirtrophenyl)prop-2-enoic acid

diffracting angle and λ is the wavelength of X-ray. From these data we have confirmed that the formation of ZnO on the ITO/ZnS substrates along with the crystallinity of ZnS coating. Huge difference were observed between the XRD patterns corresponding to the ITO-coated glass and as-deposited ZnS film on the ITO-coated glass substrate which was compared in JCPDS card no.89-4599 indicates that a very high degree of crystallinity implying the size of the ZnS particles were large. The diffraction peak at 2 θ are 32.7,35.74,37.1,which corresponds to ZnO and are in good agreement with [JCPDS card no.65-3411] Further the ZnS sharp crystalline peak at 2θ value of 25.94 (1 0 0) which exactly matches with [JCPDS card no.36-

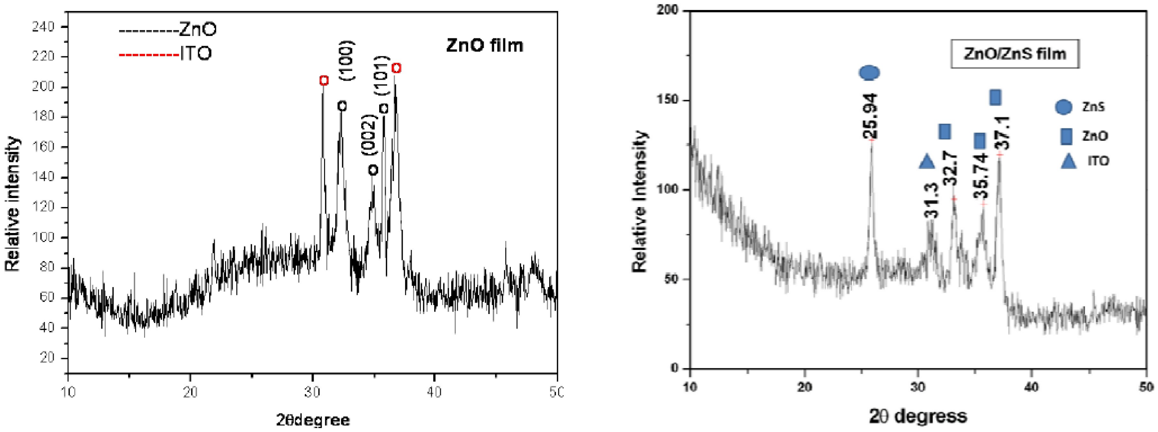

Figure 2 : XRD spectral studies of ZnO and ZnS/ZnO composite films

1450] as shown in Figure 2.

Photo-physical properties

The absorption spectra of ZnS and ZnS/ZnO composite nano crystalline films were measured without dye loading. It was observed that ZnO/ZnS composite nanostructures had higher absorption intensities over the entire wavelength range than the ZnS nanocrystalline films without a ZnO material as shown in Figure 3. This is because the optical absorption theory provides the relationship between the absorption coefficient and the photon energy, allowing the direct transitions as $(h\nu\ Eg)_{1/2}/h\nu$, which is used for band gap calculation. In Figure 4. shows a plot of $(h\nu)^2$ vs hν for ZnS and ZnS/ZnO films. The obtained nanocrystalline composite films attributed to the wider band gap of ZnS in the region 3.64 eV[43] and 3.1 eV of ZnO nanocrystalline films.

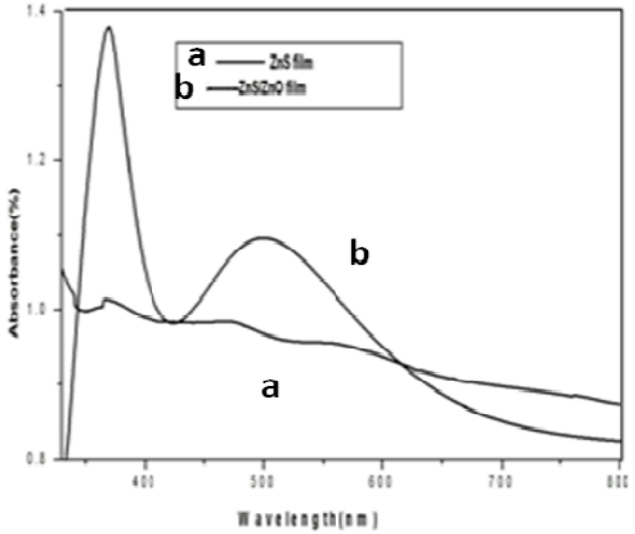

Figure 3 : Full visible absorption spectrum for both ZnS/ZnO composites and the thermally evaporated ZnS film

Entacopone intermediate [E_1] type ligands have been subjected for many studies in the area of trace metal analysis due to its potential ability to chelate with the many transition metal ions. However, these molecules have received very little attention as potential solar energy capturing pigments in dye sensitized photovoltaic cells. Intense absorption band centered in the visible range of the spectrum at ca. 442 nm and strong ability to bind with nanocrystalline ZnO semiconductor surface. The absorption spectrum of the E_1 in ethanol solution shows $\pi^* \leftarrow \pi$ transition in 442 nm region, also another band at 392 nm and 310 nm of shorter wavelength region was observed (as shown in Figure 5). The absorption spectra of both E_1-ZnO and E_1-ZnO/ZnS nanocrystalline films shows onsets of the local bands considerably red-shifted due to the oxidation potential of exited state of the adsorbed E_1 molecule and potential of the conduction band level of the ZnO semiconductor surface, energetic and geometric overlapping integral between LUMO of E_1 molecule and the density state distribution of the conduction band semiconductor and also the molecular orbital change of the E_1 molecule on the charge-transfer influences the red-shift in the broad absorption structure because of the molecular resonance structures. Hence, the obtained film considerably shows a longer wavelength when it is anchoring or chemisorbed E_1 sensitizers is as shown in Figure 6. The optical characteristics of both E_1-ZnO or E_1-ZnS/ZnO nanostructures receives more attention in this study because the dye produces excited electrons by absorbing visible light, absorbs more light when the anode is composed of ZnO/ZnS composite nanostructures. This absorption characteristic of ZnO/ZnS

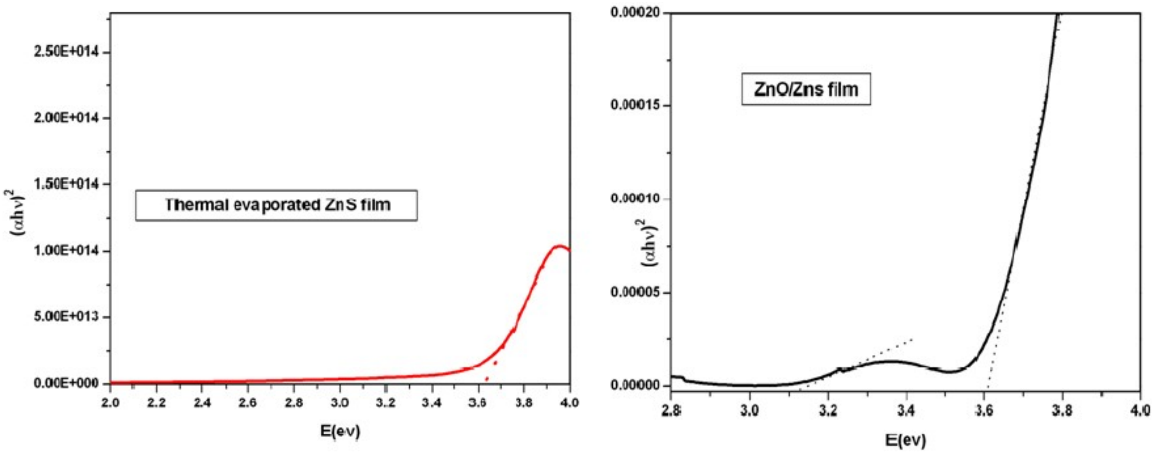

Figure 4 : Bandgap determination of ZnS/ZnO composites and the thermally evaporated ZnS film from the UV spectrum

nanostructures will be beneficial for improving the efficiency of the DSSC cells.

ATR-FTIR spectroscopy

The ATR-IR spectra (1100-1800 cm^{-1} region) of E_1-ligands adsorbed on ZnO films and free E_1 ligand are compared in Figure 7. Major IR bands of free ligands (curve A) are as follows:1682.9cm^{-1},1724.05 cm^{-1}, corresponding to C=O stretching mode; 1612 cm^{-1} for the antisymmetric stretching of CO_2; 1367.3cm^{-1} for the symmetric stretching of CO_2; 1137 cm^{-1} for C-O-H bending; 1245.2 cm^{-1} for singly bonded C-O stretching, 2238cm^{-1} for CN stretching are present in the free sample (not mentioned). The fact that both -C=O and -CO_2 stretching bands observed in our case indicates that both protonated and deprotonated carboxylic groups are present in the free sample (curve a).

The IR spectrum of E_1 ligand adsorbed on ZnO film showed a little changed in the 1100-1700 cm^{-1} region (curve b). Most prominent change is the band at 1683 cm^{-1}, 1724 cm^{-1} ν(C=O), whose intensity was greatly reduced on ZnO films and there is an intense, broad band at 1607.7cm^{-1}, which is assigned to the antisymmetric stretching of -CO_2, where the negative charge is delocalized to give two equivalent (or nearly so) C-O bonds; intense band at 1382.2 cm^{-1} corresponding to symmetric stretching of -CO_2. This indicates that the surface complexes of ligands were attached through a bidentate coordination (BC) but not monodentate coordination (MC). The band at 1137.6 cm^{-1} (C-O-H) was also absent upon adsorbing on ZnO films, which reconfirms the bidentate surface complex formation[44]. Similarly, the E_1 ligand adsorbed on ZnS/ZnO composite films were attached through a bidentate coordination due to the absence of peak intensity at 1724 cm^{-1} of C=O group and the other band at 1137.6 cm^{-1} of C-O-H group (curve c).

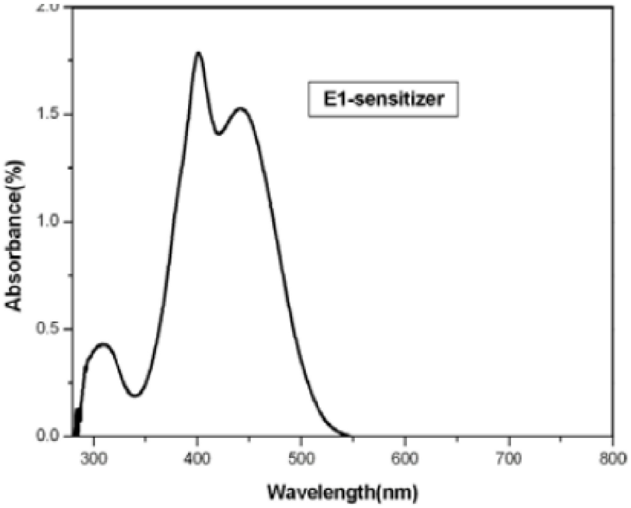

Figure 5 : UV-Visible absorbance of E_1-sensitizer

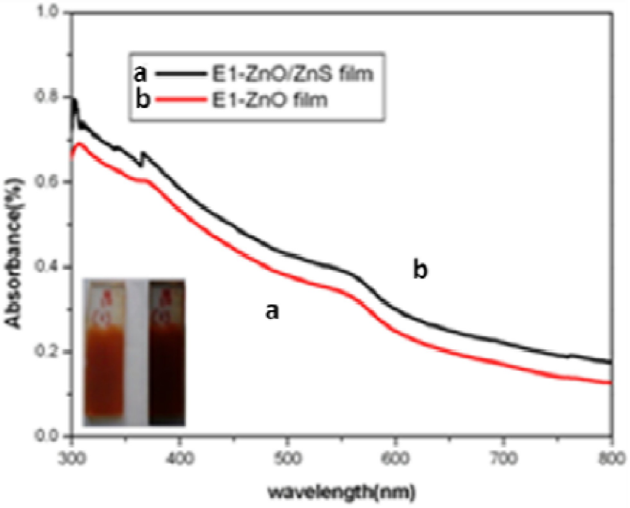

Figure 6 : UV-Visible absorbance of [a] E_1-ZnO film and [b] E_1-ZnS/ZnO composite film

Efficiency

The configuration of the photovoltaic cell is shown in Figure 8 with variation in the dye-sensitized layer in

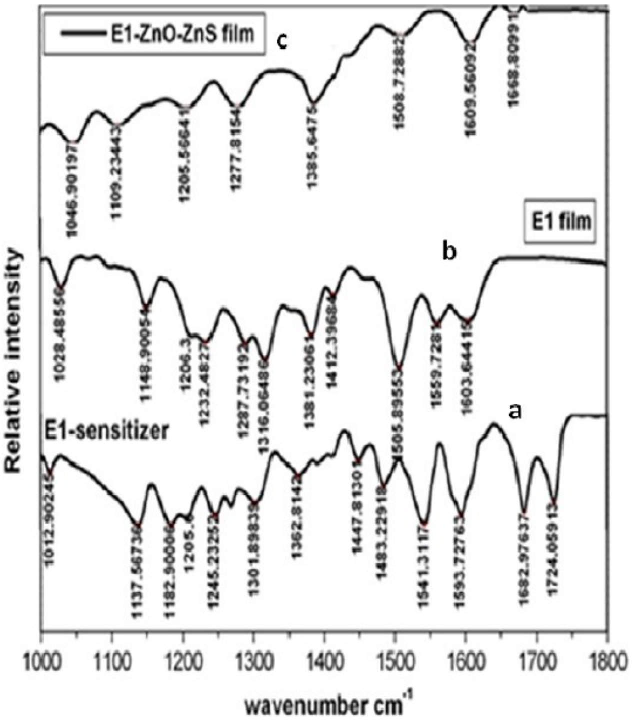

Figure 7 : ATR spectral studies of [a] E_1 sensitizer, [b] E_1 chemisorbed ZnO film and [c] E_1 chemisorbed ZnS/ZnO composite films

different cases, because the Ru-dye molecules adsorb strongly onto the metal oxide[45] and in the similar way the catacol also strongly adsorb on ZnO films, which was confirmed by ATR-IR spectral studies. The counter electrode is a thin, sputtered Pt layer onto the ITO glass and plays a role as a catalyst to facilitate the reduction of I^{-3} ions and improve the rejuvenation efficiency of the dye. The photoelectrochemical behaviors of DSSC structures were measured at an illumination intensity of AM 1.5. The photocurrent density voltage characteristics of the Cell 1 and Cell 2 are shown in Figure 8 and the related physical values, such as JSC (short-circuit current), VOC (open-circuit voltage), FF (fill factor), and η (light- to-electricity conversion efficiency), are summarized in TABLE 1. The η values can be evaluated by the equation[46].

$$\eta = Pout \backslash P_{in} = Vmax*Imax \backslash P_{in} = FF*I_{SC}*V_{OC} \backslash P_{in}$$

Where Pin is the incident light power density.

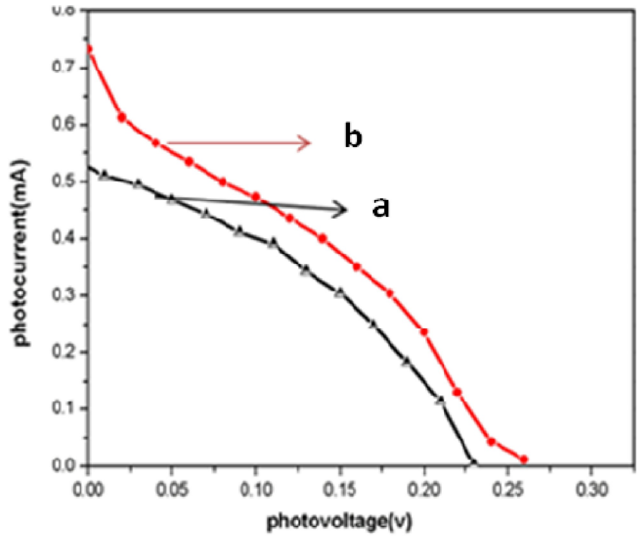

Figure 8 : I-V characteristics of the solar cells made from (a) ZnO nanostructured film (b) ZnS/ZnO nanostructured film

TABLE 1

Complex	Absorbance λ max/nm	Voc (v)	Jsc (mA cm^{-2})	FF	η(%)
E_1-ZnO	442 nm	0.23	0.528	23	0.028
E_1-ZnS/ZnO film	540 nm	0.26	0.738	28	0.055

The pure “ZnO/dye” (cell 1) was tested to have a power efficiency (η) of 0.028%, which was relatively low as compared to those (η=1.1–5.0%) reported in the literature[3]. However, a lot of parameters will affect the overall performance, including particle size, surface area, the amount of dye adsorbed, the electrolyte type, the process for dye rejuvenation, hinder the recombination process etc. In this case the Photo-excitation of these type of ligands involve ligand centered (LC) transitions and often strongly allowed transitions are well into the UV side of the spectrum. Hence, direct irradiation will cause the photodegradation of dye molecules, blocking the UV radiation results in low photocurrent conversion efficiencies. Furthermore, solar energy conversion schemes based on LC transitions do not involve an energy capture through a charge separation process. Therefore, in addition to photodegradation, charge recombination reduces the cell efficiency of photocells sensitized through an LC mechanism[47]. Hence for compared these two systems surface complexed ZnS/ZnO films shows more efficient system than the surface complexed ZnO films due to charge recombination is much less probable in composite films.

Mechanism

The mechanism of dye functions and rejuvenation is shown in Figure 9(a) in which The excited dye (D*) injects electrons into the conduction band of ZnO. Electrons are then transported through an outer circuit to the counter electrode, which reduces the I^{-3} ions back to I^-. The dye is oxidized (S^+) after the electron injection. It is rejuvenated (S) by oxidizing I^- to I^{-3}; and is then ready to be excited again.

The Voc of cell 2 is 0.26, which was greater than that of cell 1 i.e. Voc was also affected by many fac-

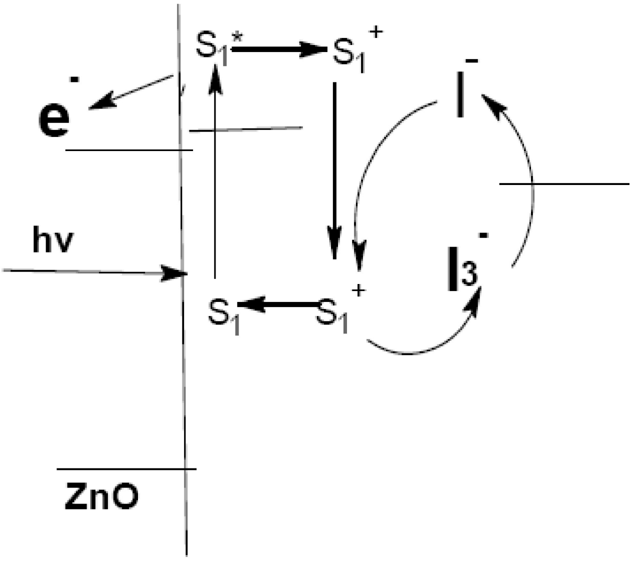

Figure 9 : (a) Relative energy diagram of a dye-sensitized photovoltaic cell with a ZnO composite thin film

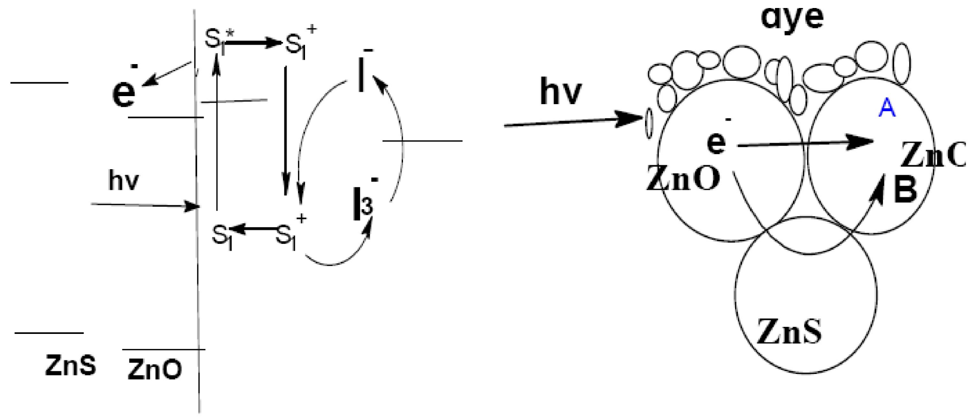

(a) (b)

Figure 10 : (a) Relative energy diagram of a dye-sensitized photovoltaic cell with a ZnS/ZnO composite thin film. (b) Illustration of the ZnS fine layer that offers a faster alternative electron pathway “B” than the original pathway “A,” which is full of barriers among ZnO particles

tors, including the type of semiconductor (Fermi-level), redox couple concentration, recombination of electrons and holes, the amount of dye, rejuvenation of the dye, etc. The ZnS/ZnO/dye composite film (in cell 2 with $\eta=0.055\%$) configuration is shown in TABLE 1.A. where the power efficiency was greater than that of the pure ZnO/dye configuration. But, according to the relative band energy diagram Figure 10a, it is unlikely that the electrons are transported faster by penetrating the ZnS layer. The electrons seems to be trapped in the ZnO phase, because it is impossible for electrons to jump up to the conduction band gap of ZnS from ZnO. In fact, the same situation is also encountered in other configuration[5,6]. One possible explanation is that the electrons are injected into the ZnO when excited and the rate determining step of electron transport in the ZnO phase is overcoming the energy barrier of ZnO, as in pathway A which is shown in Figure 10b. As electrons continue to be injected into the ZnO or ZnO with much smaller particle sizes, the conduction band of ZnO shifts upwards, which makes it possible to transport electrons from ZnO to ZnS and back again[5,6], as in pathway B shown in Figure 10b. Because of the smaller contact area (larger barrier) compared with merely ZnO particles, the transport rate of pathway B offers a much-greater contact area or increases the necking between particles, which lowers the electron charge transfer resistance and increases the power efficiency. Especially, cell 2 in Figure 5.10b, with an ultra-thin layer of 50 nm of ZnS, offers more-seamless electron transport than that of pure ZnO nanocrystalline films (cell 1).

CONCLUSIONS

This work reports the possible approach of improving the power efficiency by demonstrating feasibility of developing a composite ZnS/ZnO. The addition of ZnS might contribute a second route for electrons when they are being transported through the ZnO barriers. Electron transport is possible from ZnO to ZnS for smaller ZnO particles or continuing electron injection, which raises the Fermi-level. The maximum power efficiency in our case ZnS/ZnO composite photovoltaic cell was 0.055% which is higher than that of ZnO films [0.026 %].

ACKNOWLEDGEMENT

PNP tanks to the Department of chemistry, Kuvempu University, Karnataka, india and HRR thanks to the Principal and staff of PG Department of Physics, B.E.T, Bharathinagara, Mandya District in Karnataka State, India for permitting to carry out this research work.

REFERENCES

[1] B.O.Regan, M.Gratzel; Nature, **353**, 737 **(1991)**.
[2] M.K.Nazeeruddin, A.Kay, I.Rodicio, R.Humphry Baker, E.Muller, P.Liska, N.Vlachopoulos, M.Gratzel; J.Am.Chem.Soc., **115**, 6382 **(1993)**.

[3] A.Mills, S.Le Hunte; J.Photochem.Photobiol.A, **108**, 1 **(1997)**.

[4] N.Serpone; Res.Chem.Intermed., **20**, 953 **(1994)**.

[5] S.G.Abuabara, C.W.Cady, J.B.Baxter, C.A.Schmuttenmaer, R.H.Crabtree, G.W.V.S.Brudvig, Batista; J.Phys.Chem.C, **111**, 11982 **(2007)**.

[6] W.R.McNamara, R.C.Snoeberger, G.Li, J.M.Schleicher, C.W.Cady, M.Poyatos, C.A.Schmuttenmaer, R.H.Crabtree, G.W.Brudvig, V.S.Batista; J.Am.Chem.Soc., **130**, 14329 **(2008)**.

[7] K.Keis, J.Lindgren, S.E.Lindquist, A.Hagfeldt; Langmuir., **16**, 4688 **(2000)**.

[8] K.Keis, E.Magnusson, H.Lindstrom, S.E.Lindquist, A.Hagfeldt; Sol.Energy Mater.Sol.Cells., **73**, 51 **(2002)**.

[9] K.Tennakone, J.Bandara, P.K.M.Bandaranayake, G.R.A.Kumara, A.Konno; Jpn.J.Appl.Phys., **40**, 732 **(2001)**.

[10] **(a)** K.Tennakone, I.R.M.Kottegoda, L.A.A.De Silva, V.P.S.Perera; Semicond.Sci.Technol., **14**, 975 **(1999)**; **(b)** K.Tennakone, G.K.R.Senadeera, V.P.S.Perera, I.R.M.Kottegoda, L.A.A.De Silva; Chem.Mater., **11**, 2474 **(1999)**.

[11] A.Olea, P.J.Sebastian; Sol.Energy Mater.Sol.Cells., **55**, 149 **(1998)**.

[12] H.Horiuchi, R.Katoh, K.Hara, M.Yanagida, S.Murata, H.Arakawa, M.Tachiya; J.Phys.Chem.B, **107**, 2570 **(2003)**.

[13] N.A.Anderson, X.Ai, T.Q.Lian; J.Phys.Chem.B. **107**, 14414 **(2003)**.

[14] J.B.Asbury, N.A.Anderson, E.C.Hao, X.Ai, T.Q.Lian; J.Phys.Chem.B, **107**, 7376 **(2003)**.

[15] Y.J.Shin, J.H.Lee, J.H.Park, N.G.Park; Chem.Lett., **36**, 1506 **(2007)**.

[16] V.Ganapathy, B.Karunagaran, S.Rhee; J.Power Sources, **195**, 5138 **(2010)**.

[17] D.Wu, Z.Gao, F.Xu, Z.Shi, W.Tao, K.Jiang; Cryst.Eng.Comm., **14**, 7934 **(2012)**.

[18] M.Law, L.E.Greene, A.Radenovic, T.Kuykendall, J.Liphardt, P.D.Yang; J.Phys.Chem.B, **110**, 22652 **(2006)**.

[19] J.Qiu, M.Guo, X.Wang; ACS Appl.Mater.Interfaces, **3**, 2358 **(2011)**.

[20] Q.Zhang, B.B.Garcia, X.Zhou, Y.H.Jeong, G.Cao; Adv.Mater., **22**, 2329 **(2010)**.

[21] L.Dloczik, R.Engelhardt, K.Ernst, S.Fiechter, S.Sieber, R.Konenkamp; Appl.Phys.Lett., **78**, 3687 **(2001)**.

[22] C.Lokhande, H.M.Pathan, M.Giersig, H.Tributsch; Appl.Surf.Sci., **187**, 101 **(2002)**.

[23] R.Konenkamp, L.Dloczik, K.Ernst, C.Olesch; Physica.E, **14**, 219 **(2002)**.

[24] R.Sankapal, S.D.Sartale, C.D.Lokhande; A.Ennaoui, Sol.Energy Mater.Sol.Cells, **83**, 447 **(2004)**.

[25] H.Zhang, D.Yang, X.Ma, D.Que; Nanotechnology, **16**, 2721 **(2005)**.

[26] C.Yan, D.Xue; J.Phys.Chem.B, **110**, 25850 **(2006)**.

[27] S.K.Panda, A.Dev, S.Chaudhuri; J.Phys.Chem.C, **111**, 5039 **(2007)**.

[28] Joshua Schrier, O.Denis, Demchenko, Lin-Wang Wang; Nano Letters, **7**, 2377 **(2007)**.

[29] A.Olea, P.J.Sebastian; Sol.Energy Mater.Sol.Cells, **55**, 149 **(1998)**.

[30] C.D.Lokhande, M.S.Jadhav, S.H.Pawar; J.Electrochem.Soc., **136**, 2756 **(1989)**.

[31] C.D.Lokhande, V.S.Yermune, S.H.Pawar; J.Electrochem.Soc., **138**, 624 **(1991)**.

[32] T.Yamaguchi, Y.Yamamoto, T.Tanaka, Y.Demizu, A.Yoshida; Thin Solid Films, **375**, 281 **(1996)**.

[33] T.Orent; J.Electrochem.Soc., **141**, 1320 **(1994)**.

[34] T.Yasuda, B.P.Zhang, Y.Segawa; J.Crystal.Growth, **583**, 175 **(1997)**.

[35] S.Chakrabarti, B.Chaudhuri, S.Bhattacharjee, P.Das, B.K.Dutta; Journal of Hazardous Materials, **154**, 230 **(2008)**.

[36] J.P.Escalada, A.Pajares, J.Gianotti et al.; Chemosphere, **65**, 237 **(2006)**.

[37] C.Chen, X.Qi, B.Zhou; Journal of Photochemistry and Photobiol.A, **109**, 155 **(1997)**.

[38] D.Liu, R.W.Fessenden, G.L.Hug, P.V.Kamat; Journal of Physical Chemistry B, **101**, 2583 **(1997)**.

[39] R.Abe, K.Sayama, H.Arakawa; Journal of Photochemistry and Photobiol.A, **166**, 115 **(2004)**.

[40] K.Hara, M.Kurashige, Y.Danoh, C.Kasada, A.Shinpo, S.Suga, K.Sayama, H.Arakawa; New J.Chem., **27**, 783 **(2003)**.

[41] E.L.Mekkawi, M.S.A.Abdel Mottaleb; International Journal of Photoenergy, **7**, 95 **(2005)**.

[42] G.Srikanth, Uttam Kumar Ray, D.V.N.Srinivas Rao, P.Badarinadh Gupta, P.Lavanya, Aminul Islam; Synthetic Communications, **42**, 1359 **(2012)**.

[43] D.Kurbatov, A.Opanasyuk, S.Kshnyakina, V.Melnik, V.Nesprava; Rom.Journ.Phys., **55**, 213 **(2010)**.

[44] S.Kim, R.Finnie, John.Bartlett, L.James; Woolfrey, Langmuir, **14**, 2744 **(1998)**.

[45] K.Westermark, H.Rensmo, A.C.Lees, J.G.Vos, H.Siegbahn; J.Phys.Chem.B, **106**, 10108 **(2002)**.

[46] Y.L.Lee, Y.Zhang, J.Wang; J.Am.Ceram.Soc., **92**, 1940 **(2009)**.

[47] P.M.Jayaweera, S.S.Palayangoda, K.Tennakone; Journal of Photochemistry and Photobiol.A, **140**, 173 **(2001)**.